Convergence Analysis of Extended Kalman Filter for Sensorless Control of Induction Motor

Francesco Alonge, *Member, IEEE*, Tommaso Cangemi, Filippo D'Ippolito, *Member, IEEE*, Adriano Fagiolini, *Member, IEEE*, and Antonino Sferlazza, *Student Member, IEEE*

***Abstract*—This paper deals with convergence analysis of the extended Kalman filters (EKFs) for sensorless motion control systems with induction motor (IM). An EKF is tuned according to a six-order discrete-time model of the IM, affected by system and measurement noises, obtained by applying a first-order Euler discretization to a six-order continuous-time model. Some properties of the discrete-time model have been explored. Among these properties, the observability property is relevant, which leads to conditions that can be directly linked with the working conditions of the machine. Starting from these properties, the convergence of the stochastic state estimation process, in mean square sense, has been shown. The convergence is also explored with reference to the difference between the samples of the state of the continuous-time model and that estimated by the EKF. The results theoretically achieved have been also validated by means of experimental tests carried out on an IM prototype.**

***Index Terms*—Convergence analysis, extended Kalman filter (EKF), induction motor (IM), observability analysis, sensorless control.**

I. Introduction

A PROBLEM of great interest in real applications is that of reducing the number of sensors needed for processing a control law. This is particularly true for electrical machines because they often work in hostile environments. Motion control of systems with induction motor (IM) without speed sensor (sensorless) has been addressed by many authors, starting from either a continuous-time model (cf., e.g., [1] and the references therein) or a discrete-time model (cf., e.g., [2] and the references therein).

A crucial problem to solve for the implementation of sensorless control laws is the determination of both the rotor flux vector and the speed. This can be carried out in a deterministic setting by using observers (cf., for example, [3], [4], and the references therein) in a stochastic setting using estimators (cf., for example, [5], [6], and the references therein) or in a global way by constructing a closed-loop control law that allows the satisfaction of given design requirements, forcing three variables to converge to the rotor flux components and the speed [1]; in the last case, the computation scheme of the rotor flux and speed works only in the contest of the proposed control law.

A common approach to estimate the speed of an IM is to use an extended Kalman filter (EKF). Recently, variants of the EKF have been proposed, such as in [7], where the design and implementation of unscented Kalman filters for IM sensorless drives are investigated. In [8], the real-time implementation of a bi-input EKF estimator is described, which deals with the estimation of the whole state of the IM together with stator and rotor resistances. To cope with higher computational efforts required by these filters, alternative configurations based on Kalman filtering have been proposed [9], [10], where the complexity of the filter is reduced solving two linear least square subproblems instead of a nonlinear one. Finally, different approaches could be followed that are not based on Kalman filtering [11]–[13].

As well known, the observability property of the model is crucial for the existence of state observers or estimators. In [1], the persistency of an excitation condition, crucial for the existence of the described control law, is interpreted in terms of the observability of the IM model. In [1] and [14], the observability property of the IM continuous-time model is explored, assuming the stator current components as output. Using the rank condition, the authors pointed out that a sufficient condition for lost of observability is that the excitation voltage frequency is zero and the motor is operating at constant speed.

In [15], starting from a fifth-order model, the existence of trajectories generated by the model is also shown, corresponding to particular operation regimes, that cannot be accurately estimated by any state observer, which implies that the performance of the system is remarkably deteriorated. Recently, in [16], a unified approach to ac machine observability, based on the weak local observability concept, has been presented. However, in [16], only the deterministic continuous-time fifth-order model is considered, and the same conclusions achieved in [1] and [14] are shown.

In this paper, the observability analysis is provided, but differently from the previous works, this analysis is carried out on the sixth-order discrete-time model since our goal is to design a sixth-order discrete-time EKF for sensorless control of IM. It is shown that, starting from the discrete-time model, the observability conditions are obtained in a direct manner, by extracting only the first 3×3 minor from the nonlinear observability matrix, both at constant and varying speeds. At the best knowledge of the authors, the approach followed to determine the observability conditions is new.

Manuscript received February 10, 2014; revised May 24, 2014 and July 8, 2014; accepted August 4, 2014. Date of publication September 5, 2014; date of current version March 6, 2015.

F. Alonge, F. D'Ippolito, A. Fagiolini, and A. Sferlazza are with the Department of Energy, Information Engineering, and Mathematical Models (DEIM), University of Palermo, 90128 Palermo, Italy (e-mail: francesco.alonge@unipa.it; filippo.dippolito@unipa.it; adriano.fagiolini@unipa.it; antonino.sferlazza@unipa.it).

T. Cangemi is with Altran Italia S.p.A., 00131 Rome, Italy (e-mail: tommaso.cangemi@altran.com).

Color versions of one or more of the figures in this paper are available online at http://ieeexplore.ieee.org.

Digital Object Identifier 10.1109/TIE.2014.2355133

Moreover, the use of the EKF, considered as a means to estimate the state of a sixth-order IM–load system model, has two objectives: first, to obtain filtered stator current components, which is essential to control the IM–load system; second, to estimate stator flux components and the speed for implementing sensorless state feedback control laws [17], [18]. The estimation of the load torque indirectly allows a better estimation of the speed, but it can be also used to implement control laws based on disturbance compensation.

It is proved that the EKF estimation error is bounded in a mean square sense and bounded with probability one by using the very interesting and comprehensive approach illustrated in [19] and the convergence conditions derived in [20]. We also provide an upper bound to the estimation error of the discrete-time filter with respect to the state of the continuous-time model computed at the sampling instants.

Experimental results are shown, which are referred to tests carried out at high and low speeds. The aim is that of studying the behavior of the closed-loop system in various operating conditions. Particularly interesting is the analysis of the lost of the observability property at low speed using the new observability conditions derived here in terms of the state estimates instead of the state of the motor–load system.

This paper is organized as follows. Section II describes the model of the considered IM and its properties such as its observability. Section III deals with the observability of the IM–load model. Section IV shows the structure of the EKF, together with the convergence analysis, and a study regarding the effects of the discretization of the continuous-time model. In Section V, the results theoretically achieved are validated by means of experiments carried out on a prototype, which also shows the capabilities of the estimator for constructing sensorless control schemes. Finally, conclusions are given in Section VI.

II. Mathematical Models of the IM

A. Continuous-Time Mathematical Model

Neglecting iron losses, saturation of the electromagnetic circuit and anisotropy of the geometric structure, the continuous-time mathematical model of the IM in the stationary frame is given by (see e.g., [21])

$$\dot{z}(t) = A_c z(t) + f_c\left(z(t)\right) + B_c \nu_s(t) + g t_r(t) \tag{1}$$

where $z = (i_\alpha, i_\beta, \psi_\alpha, \psi_\beta, \omega)^T$ (see Table I), $\nu_s = (\nu_\alpha, \nu_\beta)^T$, and

$$A_c = \begin{pmatrix} -a_{11} & 0 & a_{12} & 0 & 0 \\ 0 & -a_{11} & 0 & a_{12} & 0 \\ a_{21} & 0 & -a_{22} & 0 & 0 \\ 0 & a_{21} & 0 & -a_{22} & 0 \\ 0 & 0 & 0 & 0 & -a_{33} \end{pmatrix}$$

$$f_c(z) = \begin{pmatrix} f_1\, z_4\, z_5 \\ -f_1\, z_3\, z_5 \\ -z_4\, z_5 \\ z_3\, z_5 \\ -f_3(z_1\, z_4 - z_2\, z_3) \end{pmatrix}, \quad B_c = \begin{pmatrix} f_1 & 0 \\ 0 & f_1 \\ 0 & 0 \\ 0 & 0 \\ 0 & 0 \end{pmatrix}$$

TABLE I
List of Symbols

i_α (i_β)	stator current component along α–axis (β–axis) fixed to the stator, A
ν_α (ν_β)	stator voltage component along α–axis (β–axis), V
ψ_α (ψ_β)	scaled rotor flux along α–axis (β–axis), Wb
ω	rotor speed, el. rad/s
R_s (L_s)	stator resistance (inductance), Ω (H)
L_m (L_r)	mutual (rotor) inductance, H
R_r	rotor resistance, Ω
τ_r	$\left(= \frac{L_r}{R_r}\right)$ rotor time constant, s
L_e	$\left(= L_s - \frac{L_m^2}{L_r}\right)$ stator equivalent inductance H
F	viscous friction coefficient, Nms
F_c	Coulomb friction, Nm
t_m (t_l)	motor (load) torque, Nm
J_M	inertia coefficient, Nms^2
p	pole pairs
T_s	sampling time, s
I_n	identity $n \times n$ matrix

with $g = (0, 0, 0, 0, -g_5)$, and

$$a_{11} = \frac{1}{L_e}\left(R_s + \frac{L_s - L_e}{\tau_r}\right), \quad a_{12} = \frac{1}{\tau_r\, L_e}$$
$$a_{21} = \frac{L_s - L_e}{\tau_r}, \quad a_{22} = \frac{1}{\tau_r}, \quad a_{33} = \frac{F}{J_M}$$
$$f_1 = \frac{1}{L_e}, \quad f_3 = \frac{2}{3}\frac{p^2}{J_M}, \quad g_5 = \frac{p}{J_M}.$$

Remark 1: For sensorless control, the rotor speed ω has to be estimated together with the other state variables, and consequently, it appears in the model as a state variable together with the load torque t_l that appears as an unknown disturbance. Moreover, the Coulomb friction has not been modeled due to its relay-type nature, which leads to a pulse derivative localized at $\omega = 0$, which is difficult to be interpreted when Jacobian has to be computed. However, it will be estimated by the EKF together with the load torque.

B. Continuous-Time Model for the State Estimation

To cope with the problem of Remark 1, the following dynamics are chosen for the load torque (see, e.g., [17]):

$$\dot{t}_l = 0. \tag{2}$$

Then, assuming t_l as a further state variable, the following six-order model is obtained:

$$\dot{x}(t) = \hat{A}_c x(t) + \hat{f}_c\left(x(t)\right) + \hat{B}_c\, \nu_s(t) \tag{3}$$

where $x = \left(z^T, t_l\right)^T$, and

$$\hat{A}_c = \begin{pmatrix} A_c & g \\ 0_{5\times 1} & 0 \end{pmatrix}, \quad \hat{f}_c(x) = \begin{pmatrix} f_c(z) \\ 0 \end{pmatrix}, \quad \hat{B}_c = \begin{pmatrix} B_c \\ 0_{2\times 1} \end{pmatrix}.$$

A discrete-time model corresponding to (3) can be obtained by using first-order Euler discretization. By choosing the stator current components as the system output, the discrete-time model is given by

$$\begin{aligned} x_{k+1} &= A x_k + f(x_k) + B\nu_{s,k} + \zeta_k \\ y_k &= C x_k + \xi_k \end{aligned} \tag{4}$$

where ζ_k and ξ_k are system and measurement white noises, assumed uncorrelated between them and other variables, whereas A, B, C, and $f(x_k)$ are

$$A = (I_6 + T_s\hat{A}_c), \quad f(x_k) = T_s\hat{f}_c(x_k)$$
$$B = T_s\hat{B}_c, \quad C = (I_2, 0_{2\times 4}).$$

C. Properties of the Discrete-Time Model

In the remainder of this section, we provide the following properties of the discrete-time model, whose proofs are shown in the Appendix.

Proposition 1: Function $f(\cdot)$ can be expanded around $\hat{x}_k$ as

$$f(x_k) - f(\hat{x}_k) = J(\hat{x}_k)\,(x_k - \hat{x}_k) + h(x_k, \hat{x}_k) \tag{5}$$

where $\hat{x}_k$ is a state estimate, and $J(\hat{x}_k)$ is the Jacobian of $f(\cdot)$ computed at $\hat{x}_k$, given by

$$J(\hat{x}_k) = T_s\frac{\partial f(\hat{x}_k)}{\partial \hat{x}_k} = \begin{pmatrix} 0 & 0 & 0 & \hat{f}_1\,\hat{x}_{5k} & \hat{f}_1,\hat{x}_{4k} & 0 \\ 0 & 0 & -\hat{f}_1\,\hat{x}_{5k} & 0 & -\hat{f}_1\,\hat{x}_{4k} & 0 \\ 0 & 0 & 0 & -T_s\,\hat{x}_{5k} & -T_s\,\hat{x}_{4k} & 0 \\ 0 & 0 & -T_s\,\hat{x}_{5k} & 0 & -T_s\,\hat{x}_{3k} & 0 \\ -\hat{f}_3\,\hat{x}_{4k} & \hat{f}_3\,\hat{x}_{3k} & \hat{f}_3\,\hat{x}_{2k} & -\hat{f}_3\,\hat{x}_{1k} & 0 & 0 \\ 0 & 0 & 0 & 0 & 0 & 0 \end{pmatrix}$$

and $h(\cdot,\cdot)$ contains all its nonlinearities, and it is given by

$$h(x, \hat{x}_k) = H(e_k)\,e_k \tag{6}$$

where $e_k = x - \hat{x}_k$, and

$$H(e_k) = \begin{pmatrix} 0 & 0 & 0 & 0 & \hat{f}_1\,e_{4k} & 0 \\ 0 & 0 & 0 & 0 & -\hat{f}_1\,e_{3k} & 0 \\ 0 & 0 & 0 & 0 & -T_s\,e_{4,k} & 0 \\ 0 & 0 & 0 & 0 & T_s\,e_{3,k} & 0 \\ 0 & 0 & \hat{f}_3\,e_{2k} & -\hat{f}_3\,e_{1k} & 0 & 0 \\ 0 & 0 & 0 & 0 & 0 & 0 \end{pmatrix}.$$

Proposition 2: For matrices $J(\hat{x}_k)$ and $H(e_k)$, there exist two positive constants M and α s.t.

$$\|J(\hat{x}_k)\| \le M\,\|\hat{x}_k\|, \qquad \|H(e_k)\| \le \alpha\,\|e_k\| \tag{7}$$

for all $\hat{x}_k$ and e_k, where $\|\cdot\|$ is the Euclidian norm.

From (6) and (7), it follows that, for all e_k, it occurs

$$\|h(x_k, \hat{x}_k)\| \le \alpha\,\|e_k\|^2. \tag{8}$$

Proposition 3: Function $f(\cdot)$ satisfies the following condition:

$$\|f(x_k) - f(\hat{x}_k)\| \le (M\,\|\hat{x}_k\| + \alpha\,\|e_k\|)\,\|e_k\|. \tag{9}$$

Proposition 4: Matrix $A_k = A + J(\hat{x}_k)$ satisfies the following inequality:

$$\|A_k\| \le \|A\| + M\,\|\hat{x}_k\|. \tag{10}$$

Proposition 5: Matrix A_k is affine in the variables $\hat{x}_{i,k}$ for $i = 1, \ldots, 5$.

Proposition 6: Function $\hat{f}_c(\cdot)$ satisfies the following inequality: $\|\hat{f}_c(x)\| \le 3\hat{\alpha}\|x(t)\|^2$, with $\hat{\alpha} = \alpha/T_s$.

III. Observability of the Discrete-Time Model

As well known, the observability property of a model is essential for the existence of an estimator of its state. As for the IM system, many authors provide sufficient observability conditions for the continuous-time model [14]–[16], [22]. At the best of the authors' knowledge, the observability of the discrete-time model has not been addressed, although the estimators described in many papers are based on the IM discrete-time model. In this respect, the following theorem can be proved.

Theorem 1: The nonlinear model (4) is locally weakly observable if the rotor flux vector rotates instant by instant in the stator reference frame.

Proof: According to [19], the nonlinear model (4) is weakly locally observable if the so-called rank condition is satisfied, i.e., $rank(O) = n = 6$, where matrix O is given by

$$O = \begin{pmatrix} \frac{\partial h}{\partial x}(x_k) \\ \frac{\partial h}{\partial x}(x_{k+1})\ \frac{\partial f_d}{\partial x}(x_k) \\ \vdots \\ \frac{\partial h}{\partial x}(x_{k+5})\ \frac{\partial f_d}{\partial x}(x_{k+4}) \cdots \frac{\partial f_d}{\partial x}(x_k) \end{pmatrix}$$

where $h(x_k) = Cx_k$, and $f_d = Ax_k + f(x_k) + f_1 v_{s,k}$.

Denoting with O_3 the 6×6 matrix obtained with the first three terms of O, putting $x_k = x$ and $x_{k+1} = x^+$, its determinant is given by

$$det(O_3) = -\alpha\left(x_5 - x_5^+\right)\left(x_3 x_3^+ + x_4 x_4^+\right) + \beta\left(\hat{a}_{12}^2 + \hat{f}_1^2 x_5 x_5^+\right)\left(x_3 x_4^+ - x_3^+ x_4\right) \tag{11}$$

where $\alpha = \hat{f}_1^3 T_s \hat{a}_{12} g_5$, and $\beta = \hat{f}_1^2 g_5 T_s$. Now, it is worthwhile noting that x_3 (x_3^+) and x_4 (x_4^+) are the components of the rotor flux vector $\vec{\phi}_r$ $(\vec{\phi}_r^{\,+})$ along the a- and b-axes of the stator reference frame, respectively. Consequently, denoting with ρ and ρ^+ the angles between vectors $\vec{\phi}_r$ and $\vec{\phi}_r^{\,+}$ and the a-axis, the above components are given by

$$x_3 = \phi_d\cos(\rho);\ x_3^+ = \phi_d^+\cos(\rho^+)$$
$$x_4 = \phi_d\sin(\rho);\ x_4^+ = \phi_d^+\sin(\rho^+)$$

where $\phi_d = |\vec{\phi}_r|$, and $\phi_d^+ = |\vec{\phi}_r^{\,+}|$. With these positions, $det(O_3)$ becomes

$$det(O_3) = -\alpha\phi_d\phi_d^+\left(x_5 - x_5^+\right)\cos(\rho^+ - \rho) + \beta\phi_d\phi_d^+\left(\hat{a}_{12}^2 + \hat{f}_1^2 x_5 x_5^+\right)\sin(\rho^+ - \rho). \tag{12}$$

The above equation shows that, at a constant speed $(x_5 = x_5^+)$, the rank conditions are satisfied if $\rho^+ \neq \rho\ \forall\phi_d \neq 0, \forall\phi_d^+ \neq 0$, i.e., if the rotor flux vector rotates in the stator reference frame. □

Remark 2: When the rotor flux vector is fixed in the reference stator frame, the rank condition is not satisfied, and consequently, nothing can be deduced about observability. However, it is useful to analyze the behaviors of the system in the set of states in which the rank condition fails. This set contains the states corresponding to the operating situations in which the rotor flux vector is fixed in the reference stator frame, i.e., at zero stator frequency. This frequency $\dot{\rho}$ is given by

$$\dot{\rho} = \omega + a_{21}\frac{i_q}{\phi_d}$$

where i_q is the in-quadrature stator current in the frame rotating with the rotor flux, and its discrete-time version is

$$\rho^+ - \rho = T_s\left(\omega + a_{21}\frac{i_q}{\phi_d}\right) \tag{13}$$

in which ω, i_q, and ϕ_d are evaluated at the discrete-time instant k. The above set is then obtained putting $\rho^+ = \rho$ and is given by

$$\omega + a_{21}\frac{i_q}{\phi_d} = 0. \tag{14}$$

Moreover, since the motor torque t_m generated by the motor is given by

$$t_m = f_3 i_q \phi_d$$

(14) becomes

$$\frac{a_{21}}{f_3\phi_d^2}t_m + \omega = 0 \tag{15}$$

which represents a straight line with negative slope in the $t_m - \omega$ plane crossing its origin, i.e., a line that belongs to the second and fourth quadrants of the above plane, crossing the point $t_m = 0$ and $\omega = 0$, as shown in [14].

Now, let $S = \{(\omega, t_m) : \omega \in (-x_{\min}, x_{\max})\}$ be the set of points of the trajectory (15) around the origin of the plane $t_m - \omega$, where the rank condition fails. It is useful to analyze the behaviors of the induction machine in this set S. To this regard, note that the induction machine, when it works as a motor, cannot work in the second and fourth quadrants of the plane $t_m - \omega$ at a constant speed because, in these quadrants, the motor works like a generator and produces electrical energy from the mechanical one stored in the motor, which consequently reduces its speed. Operations in these quadrants can occur during short transients due to, for example, a requirement of strong deceleration or energy recovering during braking. The only way to operate at a constant speed is to put the rotor in rotation with an auxiliary mechanical source, i.e., forcing the motor to work as an asynchronous generator.

Remark 3: Assuming the machine fluxed and at rest (i.e., $\omega = 0$ and $i_q = 0$) and applying to it an active positive load, i.e., a load able to put the rotor in rotation, an operative condition compatible with the model of the induction machine is that of a motion evolving according to the following equation:

$$\omega^+ = -\hat{a}_{33}\omega - g_5 t_l. \tag{16}$$

Then, the machine accelerates in the negative direction toward a steady-state speed equal to

$$\omega = -\frac{g_5}{(1+\hat{a}_{33})}t_l$$

without generation of motor torque. This situation cannot be observed by any model-based estimator, and consequently, it has to be treated *ad hoc*.

Remark 4: During transients, it is more difficult to verify whether the rank condition is satisfied or not. However, also in this case, it is possible to do some considerations. From (13), if $x_5^+ \neq x_5$, the rank condition is not satisfied provided that

$$tg(\rho^+ - \rho) = \hat{f}_1\hat{a}_{12}\frac{x_5 - x_5^+}{\hat{a}_{12}^2 + \hat{f}_1 x_5 x_5^+}. \tag{17}$$

It is worth noticing that, when the rotor speed is positive and increasing, $x_5 > 0$ and $x_5^+ - x_5 > 0$, (17) implies that $tg(\rho^+ - \rho) < 0$ and thus that $\rho^+ < \rho$. This is in contrast with the hypothesis that the speed is increasing. The same holds for the speed is negative and decreasing. For this reason, during the motor working condition, (17) could be satisfied only for isolated instants during braking. Equation (17) can be computed online by using the estimated variables only. However, it could be useful to verify offline if it is satisfied using the values of the variables acquired during the experiments.

IV. EKF

A. Structure of the Filter

In order to obtain an estimate $\hat{x}_k$ of the state x_k of the discrete-time system (4), the following EKF is proposed:

$$\hat{x}_{k+1} = A\hat{x}_k + f(\hat{x}_k) + B\nu_{s,k} + K_k(y_k - C\hat{x}_k) \tag{18}$$

where K_k is a gain matrix that has to be suitably updated, according to the following procedure.

The dynamics of the estimation error, i.e., $e_k = x_k - \hat{x}_k$, is given by

$$e_{k+1} = Ae_k + f(x_k) - f(\hat{x}_k) - K_k C e_k + \zeta_k - K_k\xi_k$$

which becomes, by using (5)

$$e_{k+1} = (A_k - K_k C)e_k + H(e_k)e_k + \zeta_k - K_k\xi_k. \tag{19}$$

In the previous expression, A_k is evaluated at the state $\hat{x}_k$ given by EKF. As usual, the covariance matrix of the error e_{k+1} can be obtained by neglecting the nonlinear term $H(e_k)e_k$ in (19), and it is thus given by

$$P_{k+1} = (A_k - K_k C)P_k(A_k - K_k C)^T + Q_k + K_k C P_k (A_k - K_k C)^T \tag{20}$$

where Q_k is a positive definite matrix, i.e., $Q_k \geq \underline{q}I$, with $\underline{q} > 0$, for all time instants k, s.t.

$$E\left(\zeta_k\zeta_{k'}^T\right) = Q_k\delta(k - k').$$

Minimizing P_{k+1} with respect to K_k, the following expression for K_k is obtained:

$$K_k = A_k P_k C^T\left(CP_kC^T + R_k\right)^{-1} \tag{21}$$

where R_k is a positive definite matrix, i.e., $R_k \geq \underline{r}I$, with $\underline{r} > 0$, for all time instants k, s.t.

$$E\left(\xi_k\xi_{k'}^T\right) = R_k\delta(k - k').$$

The following proposition is useful whose proof is given in the Appendix.

Proposition 7: Matrix $A_{s,k} = A_k - K_k C$ is bounded, i.e.,

$$\|A_{s,k}\| \leq S$$

for all time instants k, where S is a positive real number.

B. EKF Convergence Analysis

To prove the results of this section, the following assumptions are imposed.

Assumption 1:

- There exist real numbers $\underline{r}$, $\overline{r}$, $\underline{q}$, and $\overline{q}$, such that $\underline{q} I_6 \leq Q_k \leq \overline{q} I_6$ and $\underline{r} I_2 \leq R_k \leq \overline{r} I_2$, for all k.
- $P_0 > 0$.
- The pair (A_k, C) is uniformly observable.

Assumption 2:

- There exists a real number N such that $\|A_k\| \leq N$ for all time instants k.
- Matrix A_k is invertible for all time instants k.

The problem is to show that, under suitable conditions, the stochastic process e_k is bounded. To this purpose, recall from [19, Lemma 4.2] that there exist real numbers $\underline{p}$ and $\overline{p}$, such that the following inequalities:

$$\underline{p} I_6 \leq P_k \leq \overline{p} I_6 \tag{22}$$

hold under Assumption 1.

Remark 5: Only the third item of Assumption 1 needs some discussion. First of all, it should be noticed that the observability property of the model, discussed in Section III, is a necessary condition for the existence of an estimator for the model itself. A sufficient condition for the existence of an estimator is the uniform observability of the couple (A_k, C). Moreover, as it is easy to verify, the rank condition implies the uniform observability of the pair (A_k, C). Indeed, matrix O_3 (cf., Theorem 1), particularized with the state estimates instead of true state, is equal to matrix Q_o, given by

$$Q_o = \begin{pmatrix} C \\ CA_k \\ CA_{k+1}A_k \end{pmatrix}. \tag{23}$$

It follows that the conditions of uniform observability are the same to those of the motor model, particularized with the state estimates, i.e., the estimated rotor flux rotates, at a constant speed, whereas the condition is lost if (17) is satisfied with the estimated variables instead of the motor ones. However, the test of uniform observability can be carried out only during the experiments. This will be further discussed later, in Section V.

The first main result can be now stated on the convergence of the proposed EKF.

Theorem 2: Consider the discrete-time IM's model in (4) and the EKF described in (18). Under the conditions of Assumptions 1 and 2, the estimation error e_k is exponentially bounded in mean square and bounded with probability one if the initial estimation error satisfies the following inequality:

$$\|e_0\| \leq \epsilon = \min\left(\frac{2S}{\alpha}, \frac{\beta \underline{p}}{8S\alpha\overline{p}}\right)$$

where $\beta > 0$ is a suitable constant.

Proof: Consider the candidate Lyapunov function

$$V(e_k) = e_k^T P_k^{-1} e_k. \tag{24}$$

Note that $V(0) = 0$ and $(1/\overline{p})\|e_k\|^2 \leq V(e_k) \leq (1/\underline{p})\|e_k\|^2$, for $e_k \neq 0$, since P_k is positive definite and upper bounded. It needs to find an upper bound for the conditional expectation of $V(e_{k+1})$ given e_k. Direct computation gives

$$\begin{aligned} &E\left(V(e_{k+1})|e_k\right) - V(e_k) \\ &\quad = E\left(\Gamma_k(e_k)e_k + n_k\right)^T P_{k+1}^{-1}\left(\Gamma_k(e_k)e_k + n_k\right)) - V(e_k) \end{aligned}$$

where $\Gamma_k(e_k) = A_{s,k} + H(e_k)$, and $n_k = \xi_k - K_k\zeta_k$. Recall from [19] that, under Assumptions 1 and 2, the following inequality holds:

$$e_k^T A_{s,k}^T P_{k+1}^{-1} A_{s,k} e_k - e_k^T P_k^{-1} e_k \leq -\beta V(e_k) \tag{25}$$

for some $\beta \in (0,1)$. By noticing that $A_{s,k}$, P_k^{-1}, $H(e_k)$, and e_k are independent of n_k and by using (25), it is obtained

$$\begin{aligned} E\left(V(e_{k+1})|e_k\right) - V(e_k) \leq &-\beta V(e_k) + 2e_k^T A_{s,k}^T P_{k+1}^{-1} H(e_k) e_k \\ &+ e_k^T H^T(e_k) P_{k+1}^{-1} H(e_k) e_k + E\left(n_k^T P_{k+1}^{-1} n_k\right). \end{aligned}$$

Under the same assumptions and noticing that $\|C\| = 1$, there exists a positive number γ, given by

$$\gamma = \frac{6\overline{q}}{\underline{p}} + \frac{2N^2\overline{p}^2\overline{r}}{\underline{p}\underline{r}^2}$$

s.t. $E(n_k^T P_{k+1}^{-1} n_k) \leq \gamma$ (see again [19, Lemma 3.3]). Hence, it is possible to write

$$E\left(V(e_{k+1})|e_k\right) - V(e_k) \leq -\beta V(e_k) + \delta(e_k) + \gamma \tag{26}$$

with

$$\delta(e_k) = 2\frac{\alpha S}{\underline{p}}\|e_k\|^3 + \frac{\alpha^2}{\underline{p}}\|e_k\|^4 = \frac{\alpha}{\underline{p}}\|e_k\|^3\left(2S + \alpha\|e_k\|\right).$$

Moreover, for $\|e_k\| \leq \epsilon' = 2S/\alpha$, it results $\alpha\|e_k\| \leq 2S$, and thus

$$\delta(e_k) \leq 4\frac{S\alpha}{\underline{p}}\|e_k\|^3.$$

Finally, for $\|e_k\| \leq \epsilon = \min(\epsilon', \beta\underline{p}/8S\alpha\overline{p})$, it follows that

$$\delta(e_k) \leq 4S\alpha\frac{\overline{p}}{\underline{p}}\|e_k\|\frac{1}{\overline{p}}\|e_k\|^2 < \frac{\beta}{2\overline{p}}\|e_k\|^2 \leq \frac{\beta}{2}V(e_k).$$

Inserting the last equation into (26) yields

$$E\left(V(e_{k+1})|e_k\right) - V(e_k) \leq -\beta' V(e_k) + \gamma \tag{27}$$

for $\|e_k\| \leq \epsilon$, where $\beta' = 0.5\beta$. Indeed, as in [19, Lemma 3.3], it can be assumed that, for the noise upper bound γ, there exists $\tilde{\epsilon} < \epsilon$ s.t.

$$\gamma = \frac{\beta'\tilde{\epsilon}^2}{\overline{p}}$$

whereas, for all e_k s.t. $\tilde{\epsilon} \leq \|e_k\| \leq \epsilon$, it results that

$$\gamma \leq \frac{\beta'\|e_k\|^2}{\overline{p}} \leq \beta' V(e_k)$$

and thus, the right member of (27) is less than or equal to zero. From (27), it is obtained that [20]

$$E\left(V(e_{k+1})|e_0\right) \leq \gamma \sum_{i=0}^{k-1} (1-\beta')^i + (1-\beta')^k V(e_0) \quad (28)$$

and then

$$E\left(\|e_k\|^2|e_0\right) \leq \frac{\overline{p}}{\underline{p}}(1-\beta')^k \|e_0\|^2 + \gamma\overline{p}\sum_{i=0}^{k-1}(1-\beta')^i. \quad (29)$$

Now, observe that

$$\sum_{i=0}^{k-1}(1-\beta')^i < \sum_{i=0}^{\infty}(1-\beta')^i = \frac{1}{\beta'}$$

assuming that $\|e_0\| \leq \epsilon$, $\|e_k\|$ remains exponentially bounded in mean square and bounded with probability one. Moreover, it results

$$\lim_{x\to\infty} E\left(\|e_k\||e_0\right) = \tilde{\epsilon}.$$

■

Remark 6: The items of Assumption 2, regarding matrix A_k, need some discussion. As already said, matrix A_k depends on the estimated state $\hat{x}_k$, according to the following equation:

$$\begin{aligned}|A_k| = &-\hat{a}_{33}\left(\mu_1^2 + \mu_2^2\hat{x}_{5k}^2\right) + -\hat{f}_3\mu_2^2(\hat{x}_{2k}\hat{x}_{3k} - \hat{x}_{1k}\hat{x}_{4k})\hat{x}_{5k} \\ &+ \hat{f}_3\mu_1\left(\hat{f}_1\left(\hat{x}_{3k}^2 + \hat{x}_{4k}^2\right) - \mu_2(\hat{x}_{1k}\hat{x}_{3k} - \hat{x}_{2k}\hat{x}_{4k})\right) \quad (30)\end{aligned}$$

with $\mu_1 = \hat{a}_{11}\hat{a}_{22} - \hat{a}_{12}\hat{a}_{21}$ and $\mu_2 = \hat{a}_{11}T_s - \hat{a}_{21}\hat{f}_1$ and

$$\begin{aligned}&\hat{a}_{11} = -(1-T_s a_{11}), \quad \hat{a}_{22} = -(1-T_s a_{22}) \\ &\hat{a}_{33} = -(1-T_s a_{33}), \quad \hat{a}_{12} = T_s a_{12}, \quad \hat{a}_{21} = T_s a_{21} \\ &\hat{f}_1 = T_s f_1, \quad \hat{f}_3 = T_s f_3.\end{aligned}$$

With the sampling frequencies usually chosen (10–20 kHz), the coefficients of (30) satisfy inequalities $\hat{a}_{33} < 0$, $\mu_2 < 0$, and $\mu_1 > 0$. From (30), it is difficult to infer about the existence of the inverse of matrix A_k because it depends on the estimated state. Then, the condition $|A_k| \neq 0$ can be checked only after computation of $\hat{x}_k$, which can be carried out either online, i.e., during the experiments (see Section V), or offline using data acquired during the experiments themselves. Moreover, if the state estimates are near to the true ones, some physical considerations can be made about the terms of (30). In fact, in this hypothesis, the second term is proportional to the mechanical power generated by the motor, and the third term is the sum of a term proportional to the square of the rotor flux and a term proportional to the product of the rotor flux and the direct current producing the rotor flux. The first and third terms are positive, whereas the second term can be positive or negative. In this situation, it can be said that $|A_k| \neq 0$ for $\hat{x}_{5,k} = 0$, and matrix A_k could be singular but in isolated instants of time. With reference to the required bound of the norm of $\|A_k\|$, it can be checked during the experiments by computing the maximum singular value of A_k and verifying if it is bounded or not (see Section V).

C. Effect of the Euler Discretization

The previous convergence analysis shows that the estimation error of the IM's discrete-time model is bounded. In this section, the accuracy of the proposed filter is proved by verifying that it is also bounded the difference between the state of the continuous-time model, computed at the sampling times, and the state estimated by the EKF. This analysis is aimed to highlight the effects produced by the discretization process on the accuracy of the discrete-time model, i.e., effects whose nature is deterministic. In this contest, the analysis will be carried out in a deterministic setting, i.e., by neglecting the terms relative to the system and measurement noises.

To this purpose, consider the solution $x(t)$ of the dynamic system in (3) and its corresponding Taylor expansion computed around $x(t_0)$, given by

$$\begin{aligned}x(t) = &\, x(t_0) + \dot{x}(t)|_{t_0}(t-t_0) \\ &+ \cdots + \frac{x^{(n)}|_{t_0}}{n!}(t-t_0)^n + \frac{x^{(n+1)}(t)|_{t_\lambda}}{(n+1)!}(t-t_0)^{n+1} \quad (31)\end{aligned}$$

where $t_\lambda \in (t_0, t)$, and the last term of the equation is the Lagrange remainder.

Putting $t_0 = t_k$ and $t = t_{k+1} = t_k + T_s$, (31) can be specialized for $n = 1$, which gives the following Euler discretization:

$$x(t_{k+1}) = x(t_k) + T_s\dot{x}(t)|_{t_k} + \frac{T_s^2}{2}\ddot{x}(t)|_{t_{\lambda_k}} \quad (32)$$

where $t_{\lambda_k} \in (t_k, t_{k+1})$. From (4), it results

$$\dot{x}(t)|_{t_k} = Ax(t_k) + f\left(x(t_k)\right) + B\nu_s(t_k)$$

and direct computation of the second temporal derivative gives

$$\ddot{x}(t)|_{t_{\lambda_k}} = A\dot{x}\left(t_{\lambda_k}\right) + \frac{d}{dt}f\left(x(t)\right)|_{t_{\lambda_k}} = \tilde{A}\dot{x}\left(t_{\lambda_k}\right)$$

$$\tilde{A} = A + \left.\frac{\partial f(x)}{\partial x}\right|_{x(t_{\lambda_k})}.$$

Consequently, (32) can be written as

$$x(t_{k+1}) = x(t_k) + T_s\left(Ax(t_k) + f\left(x(t_k)\right) + B\nu_s(t_k)\right) + \sigma_k$$

where $\sigma_k = (T_s^2/2)\ddot{x}(t)|_{t_{\lambda_k}}$ is the truncation error at t_{k+1} given the values of the variables at t_k.

According to (18), the structure of the proposed EKF is given by

$$\hat{x}_{k+1} = \hat{x}_k + T_s\left(A\hat{x}_k + f(\hat{x}_k) + B\nu_s(t_k)\right) + K_k\left(y(t_k) - C\hat{x}_k\right). \quad (33)$$

The dynamics of the discretization error $\epsilon_k = x(t_k) - \hat{x}_k$ between the state x of the continuous-time model, sampled at the continuous time t_k, and the state $\hat{x}_k$, estimated by the EKF at the discrete step k, is

$$\epsilon_{k+1} = (I + AT_s - K_kC)\epsilon_k + T_s\left(f\left(x(t_k)\right) - f(\hat{x}_k)\right) + \sigma_k$$

which, by means of (5), can be simplified as

$$\epsilon_{k+1} = A_{s,k}\epsilon_k + H(\epsilon_k)\epsilon_k + \sigma_k. \quad (34)$$

Equation (34) is analogous to (19), except for the presence of the deterministic term σ_k instead of the noise terms. It follows that the convergence analysis of ϵ_k can be carried out by means of the classical Lyapunov method for discrete-time models.

It is then possible to prove the following.

Theorem 3: Under the hypothesis on the second derivative of the continuous-time model's solution, $x(t)$ and the sampling time T_s, given by

$$\ddot{x}(t)T_s^2 \leq 2\bar{\sigma}, \quad \text{for all } t \tag{35}$$

the norm of the discretization error ϵ_k exponentially converges to a value that is upper bounded by the quantity $\underline{\delta} = \sqrt{2\overline{\sigma}^2\overline{p}/\underline{p}\overline{\beta}'}$, where $\overline{\beta}'$ will be defined later.

Proof: Consider the candidate Lyapunov function

$$V(\epsilon_k) = \epsilon_k^T L_k^{-1} \epsilon_k$$

where L_k is a symmetric positive definite matrix, which is assumed here as the solution of the previous considered Riccati equation. The forward difference of $V(\epsilon_k)$ satisfies the following inequality:

$$V(\epsilon_{k+1}) - V(\epsilon_k) \leq -\overline{\beta}V(\epsilon_k) + 2\epsilon_k^T A_{s,k}^T P_{k+1}^{-1} H(\epsilon_k)\epsilon_k + 2\epsilon_k^T A_{s,k}^T P_{k+1}^{-1}\sigma_k + \epsilon_k^T H^T(\epsilon_k) P_{k+1}^{-1} H(\epsilon_k)\epsilon_k + \sigma_k^T P_{k+1}^{-1}\sigma_k.$$

By using Propositions 2 and 7, this equation becomes

$$\begin{aligned} V(\epsilon_{k+1}) - V(\epsilon_k) &\leq -\overline{\beta}V(\epsilon_k) + \frac{1}{\underline{p}}\left(2S\overline{\sigma}\|\epsilon_k\| + \overline{\sigma}^2 + \alpha^2\|\epsilon_k\|^4 + 2S\alpha\|\epsilon_k\|^3\right) \\ &= -\overline{\beta}V(\epsilon_k) + \frac{\alpha}{\underline{p}}\|\epsilon_k\|^3\left(2S + \alpha\|\epsilon_k\|\right) + \frac{\overline{\sigma}}{\underline{p}}\left(2S\|\epsilon_k\| + \overline{\sigma}\right) \end{aligned}$$

under the assumptions $|\sigma_k| \leq \bar{\sigma}$, for all k. Assuming that

$$\|\epsilon_k\| \leq \overline{\delta} = \min\left(\frac{2S}{\alpha}, \frac{\overline{\sigma}}{2S}, \frac{\overline{\beta}'}{4S\alpha}\frac{\underline{p}}{\overline{p}}\right)$$

the previous inequality becomes

$$V(\epsilon_{k+1}) - V(\epsilon_k) \leq -\overline{\beta}'V(\epsilon_k) + \overline{\gamma} \tag{36}$$

where $\overline{\gamma} = 2(\bar{\sigma}^2/\underline{p})$. Following the same procedure as in Theorem 2, it can be proved that there exists a positive quantity $\underline{\delta} < \overline{\delta}$, with $\underline{\delta}^2 = \overline{\gamma}\overline{p}/\overline{\beta}'$, s.t. for $\underline{\delta} < \|\epsilon_k\| \leq \overline{\delta}$ it results

$$\overline{\gamma} \leq \frac{\overline{\beta}'}{\overline{p}}\|\epsilon_k\|^2 \leq \overline{\beta}'V(\epsilon_k).$$

It follows that the second member of (36) is negative or null, and for $\underline{\delta} \leq \|\epsilon_0\| \leq \overline{\delta}$, $\|\epsilon_k\|$ is exponentially bounded and converges to a value upper bounded by $\underline{\delta}$. ■

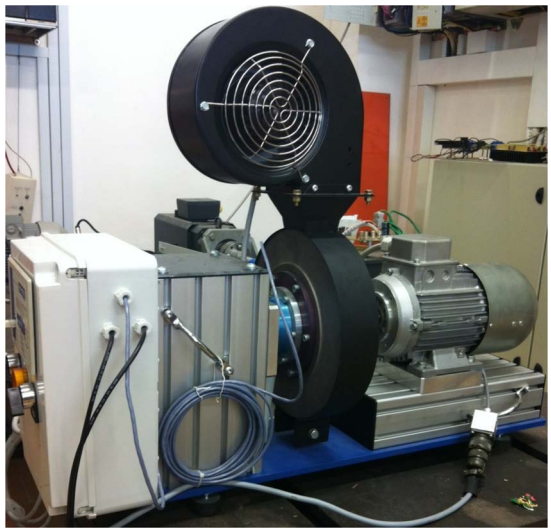

Fig. 1. Motor–brake system.

TABLE II
MOTOR PARAMETERS

L_s	$0.5236H$	J_M	$0.0056Nms^2$
L_e	$0.043H$	F_c	$1.68Nm$
R_s	15.68Ω	F	$0.0023Nms$
τ_r	$0.0669s$	p	2

TABLE III
RATED DATA OF THE MOTOR

Rated power	$750W$	Rated speed	$1410rpm$
Rated voltage	$380V$	Rated torque	$5Nm$
Rated frequency	$50Hz$	Pole pairs	2

V. EXPERIMENTS

Experiments have been carried out with the aim of validating the above described EKF. The prototype constructed for this purpose consists of a 750-W IM and a powder brake system shown in Fig. 1. The IM is driven by a source voltage inverter, and a microcontroller DSpace 1103 is used to implement both EKF and the control law. In particular, the control law is designed according to a field-oriented approach and consists in a cascade controller with four PI control loops, two inner current loops, and two outer rotor flux and speed loops [23]. (An alternative control scheme for sensorless IM drives has been recently proposed in [24].) The PI controllers are designed to obtain a bandwidth of 10 Hz for speed and rotor flux loops and 40 Hz for current loops. An anti-wind-up scheme is designed for the speed control loop. The modules of stator current and voltage vectors are constrained to $I_{s,\mathrm{MAX}} = 7$ A in order to avoid damage of the machine, i.e., $V_{s,\mathrm{MAX}} = 0,866\ \mathrm{V_{BUS}}$. The measured variables are the two stator currents given by two Hall effect transducers. All the aforementioned four control loops are closed through the proposed EKF. However, in order to compare estimated and measured speeds, the speed is also acquired by means of a 1024-ppr incremental encoder.

The whole controller, including the proposed estimator, is processed at 12 kHz.

The parameters and the rated data of the motor are shown in Tables II and III, respectively.

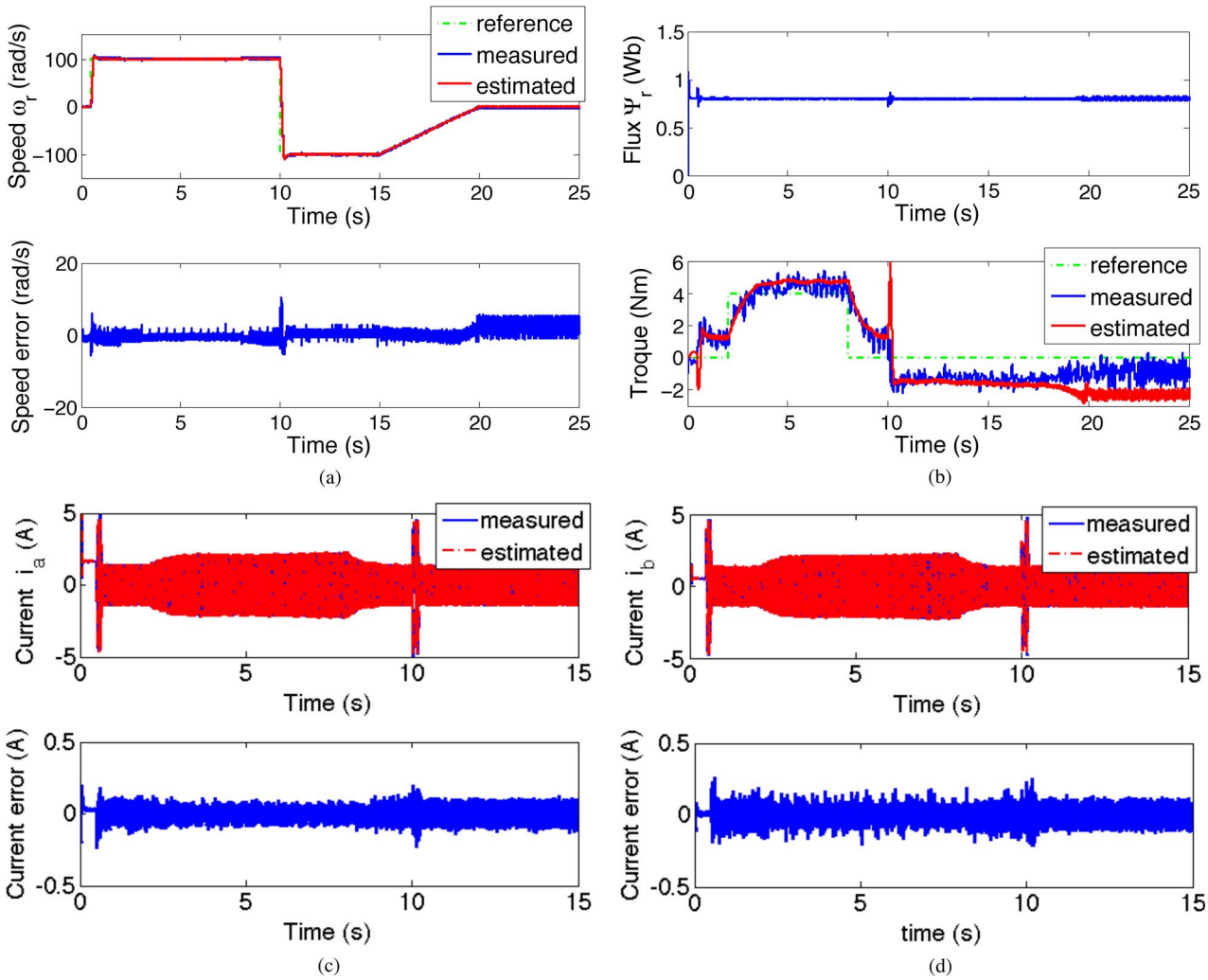

Fig. 2. Experimental waveform during a test at nominal speed and load and with speed reversal.

Matrices Q and R, necessary for processing EKF, have been obtained by means of a suitable preliminary experiment so that the estimated stator currents produced by EKF track the measured ones. In particular, matrix R has been chosen equal to the identity matrix $I_{2\times 2}$, and Q has been parameterized as $Q = \mathrm{diag}(q_{11}I_{2\times 2}, q_{22}I_{2\times 2}, q_{33}, q_{44})$, with $q_{11} = 8.149 \times 10^{-2}$, $q_{22} = 4.68 \times 10^{-5}$, $q_{33} = 2.619 \times 10^{-2}$, and $q_{44} = 11.363 \times 10^{-5}$.

The results of some experiments are shown in Figs. 2–6. Fig. 2 shows the waveforms of angular speed, stator currents, rotor flux, and torque during a suitable test at a maximum speed of 100 rad/s and rated load, whereas Fig. 3 shows the waveforms of angular speed, stator currents, rotor flux, and torque during a test at very low speed of 3 rad/s and rated load. In particular, Fig. 2 shows the closed-loop responses corresponding to a trapezoidal reference speed when the motor is fluxed at 0.8 Wb at $t = 0$, starts at $t = 0.5$ s with a step reference speed of $\omega_r = 100$ rad/s, then at $t = 10$ s, there is a speed reversal, and finally, the speed is put to zero by means of a ramp. A load torque of 4 Nm is applied at 2 s and removed at 8 s. Fig. 3 shows the closed-loop responses corresponding to a very low speed test, which is a classical critical condition in all the model-based observers/estimators for sensorless control of induction machines, when the motor is fluxed at 0.8 Wb at $t = 0$, then starts at $t = 0.5$ s with a step reference speed of $\omega_r = 3$ rad/s. The load torque of 4 Nm is applied at 2 s and removed at 8 s.

Finally, Fig. 4 is shown with the aim of verifying the observability conditions during the above two tests. More precisely, both members of (17) are computed online using, obviously, the estimated variables instead of the actual ones. This corresponds to evaluate the observability property of the couple (A_k, C), as required from Assumption 1 in Section IV-B. In particular, in Fig. 4(a) and (b), the waveforms of the first and second members of (17) are shown corresponding to the tests in Figs. 2 and 3, respectively.

From Figs. 2 and 3, a good behavior of the estimator is shown in all operating conditions. In fact, the observer is capable to track all state variables, and the controller with feedback from estimated variables is capable to cope with the disturbance very well.

Examination of Fig. 4(a) shows that (17) is satisfied near zero speed before starting with the machine fluxed ($t < 0.5$ s), when the speed passes through zero during speed reversal (about $t = 10$ s), and then when speed is forced again to zero ($t > 18$ s). When the rank condition is lost just either in isolated instants or in a few instants of time, estimates given by EKF are careful, but

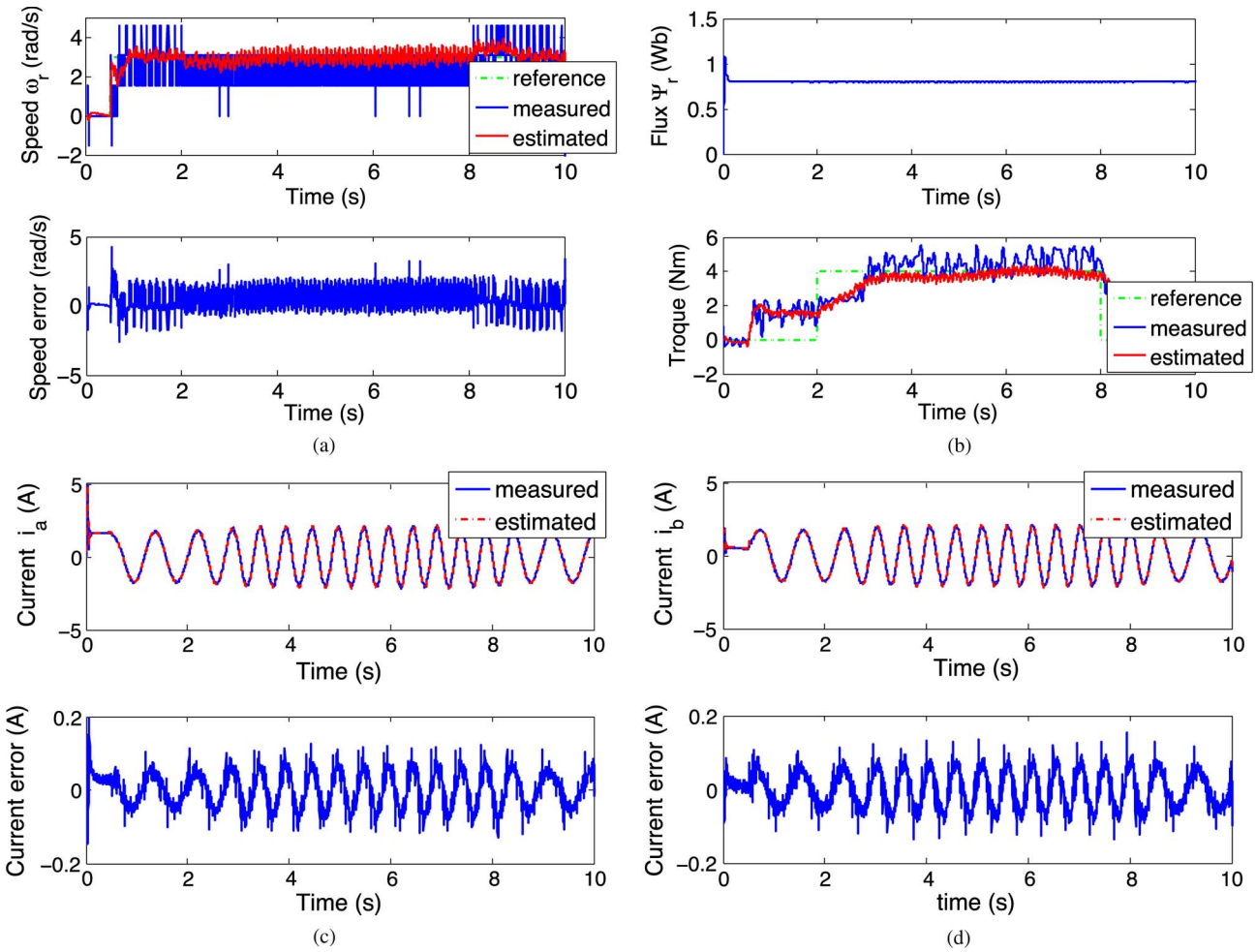

Fig. 3 Experimental waveform during a test at low speed and with nominal load.

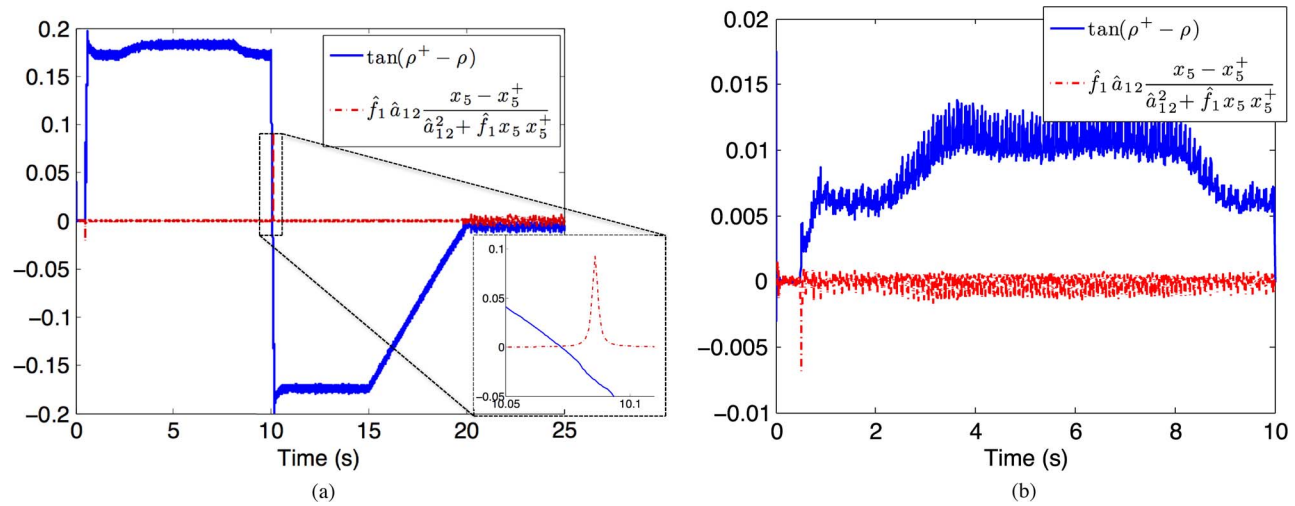

Fig. 4 Observability condition (17) computed at the sampling instants for the test at Fig. 2(a) and for the test at Fig. 3(a).

when the rank condition is lost in several instants, the behavior of EKF deteriorates. This is shown also in Fig. 2(a)–(d), where the closed-loop system, after few instants in which it remains at rest, displays a speed oscillating from about -0.5 rad/s to about 2.5 rad/s, and also the estimated load torque presents an error. While for isolated instants, i.e., during the speed reversal, the lost of rank does not represent a big problem. Fig. 4(b) shows that also for very low speed, after a time interval before and at the beginning of the starting, in which (17) is satisfied, indeed the system is capable to track the reference speed also in presence of the torque load.

Finally, from the above analysis, it is useful to note that (17) represents a strong instrument to analyze when the observer and, therefore, the whole control system are working correctly.

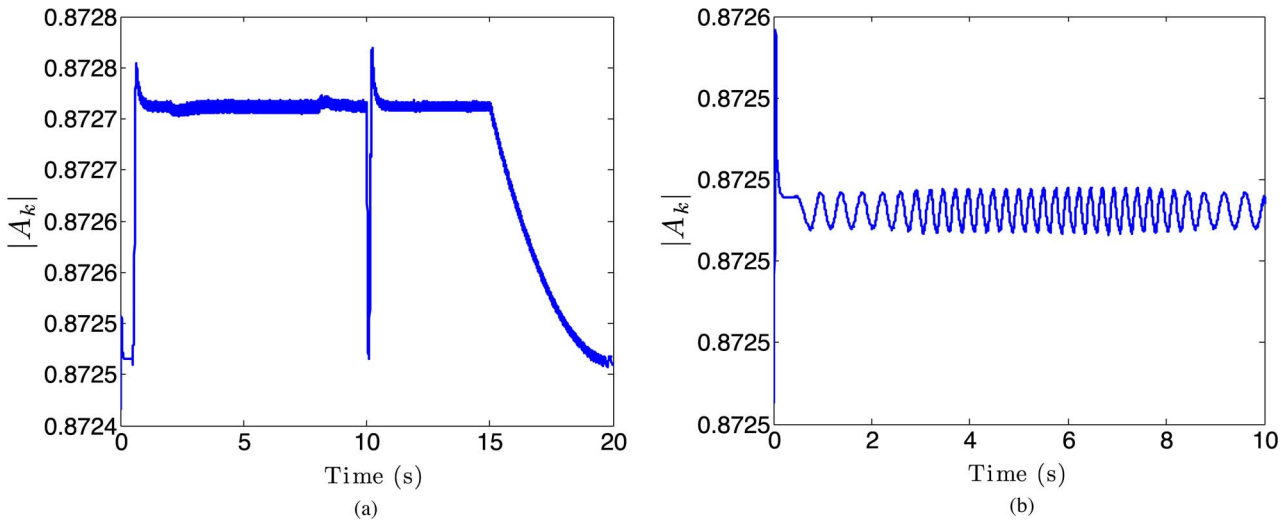

Fig. 5. Set of values of $|A_k|$ computed at the sampling instants for the test at Fig. 2(a) and for the test at Fig. 3(a).

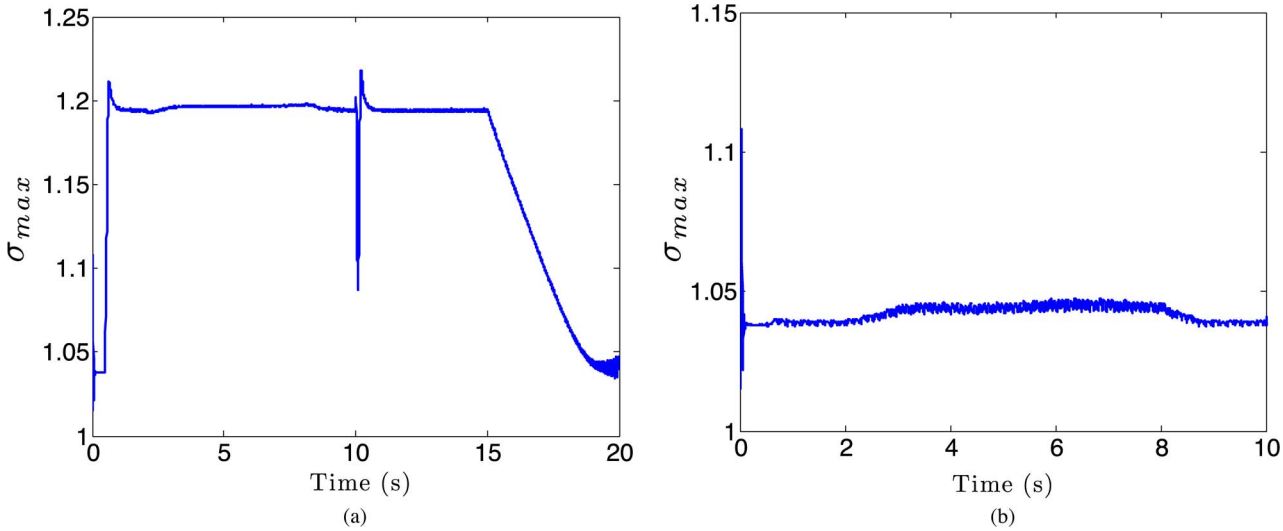

Fig. 6 Set of values of the maximum singular value of A_k, $\sigma_{\max}(A_k)$ computed at the sampling instants, for the test at Fig. 2(a) and for the test at Fig. 3(a).

In Fig. 5, the set of values of $|A_k|$ is displayed, computed at the sampling instants, at the above discussed low- and high-speed experiments. The shape of the corresponding waveforms shows that matrix A_k is always nonsingular. In particular, it appears that the computed minimum value is greater than the term $-\hat{a}_{33}\mu_1$ of (30). This fact has been confirmed in many other experiments carried out in various operating conditions.

In Fig. 6, the set of values of the maximum singular value of A_k, $\sigma_{\max}(A_k)$, is displayed, computed at the sampling instants, at low- and high-speed experiments. As well known, it results $\|A_k\| = \sigma_{\max}(A_k)$, and consequently, if $\sigma_{\max}(A_k)$ is bounded, it is possible to verify the first requirement of Assumption 2. In Fig. 6, it appears that matrix A_k is bounded in norm, and the bound diminishes with the operative speed range.

VI. Conclusion

Through the analysis carried out in this paper, interesting properties of the discrete-time version of the IM model have been shown. This allows giving convergence guarantees of the state estimates of the motor–load discrete-time model in a mean square sense and with probability one. The study effected in this paper suggests some interesting comments. First of all, the observability checking carried out on the motor–load discrete-time model leads to conditions more understandable and simple to be used than those obtained from the continuous-time model. Second, the observability of the IM model is a necessary condition for the existence of a state estimator, whereas the sufficient condition is the uniform observability of its linearized model. Third, the time-varying nature of the linearized model, obtained at each sampling time, needs to check some properties, either online or offline, such as uniform observability, existence of the inverse of a matrix, and boundedness in the norm of a matrix. The effects of the discretization are also analyzed in a deterministic setting, showing, along with the observability and convergence analysis, a good theoretical treatment of the EKF when it is used to estimate the state of an IM. Experimental findings are displayed with the aim of verifying the aforementioned properties and validating the capabilities of the estimator in sensorless control schemes in both high and low speeds.

APPENDIX
PROOFS OF THE PROPOSITIONS

Proof of Proposition 1: By inspection of the model (4). □

Proof of Proposition 2: By inspection, matrix $J(\hat{x}_k)$ can be written as $J(\hat{x}_k) = \sum_{i=1}^{5} J_i \hat{x}_{i,k}$, where $J_1 = (0,0,0,q_1,0,0)$, $J_2 = (0,0,-q_1,0,0,0)$, $J_3 = (0,-q_1,0,0,q_3,0)$, $J_4 = (q_1,0,0,0,q_4,0)$, and $J_5 = (0,0,q_3,q_4,0,0)$, with $q_1 = T_s(0,0,0,0,-f_3,0)^T$, $q_3 = T_s(0,-f_1,0,0,0,0)^T$, and $q_4 = T_s(f_1,0,-1,0,0,0)^T$. Then, we have

$$\|J(\hat{x}_k)\| \leq \sum_{i=1}^{5} \|J_i\| |\hat{x}_{i,k}| \leq \sum_{i=1}^{5} \|J_i\| \|\hat{x}_k\|. \tag{A-1}$$

Moreover, being $\|J_1\| = \|J_2\| = T_s f_3$, $\|J_3\| = \|J_4\| = \max\{T_s f_3, T_s\sqrt{1+f_1^2}\}$, $\|J_5\| = T_s\sqrt{1+f_1^2}$, we obtain (6) with $M = T_s(2f_3 + \sqrt{1+f_1^2} + 2\max\{f_3, \sqrt{1+f_1^2}\})$.

As for matrix $H(e_k)$, recall that

$$\|H(e_k)\| = \sqrt{\bar{\sigma}\left(H(e_k)^T H(e_k)\right)} = \sqrt{\bar{\sigma}\left(\tilde{H}(e_k)\right)}$$

where $\bar{\sigma}(\tilde{H})$ denotes the maximum singular value of matrix $\tilde{H}$. It is easy to verify that the set of singular values of $\tilde{H}$ is given by

$$\left\{0,0,0,0, T_s^2 f_3^2 \left(e_{1,k}^2 + e_{2,k}^2\right), T_s^2\left(1+f_1^2\right)\left(e_{3,k}^2 + e_{4,k}^2\right)\right\}$$

and, consequently, we have

$$\|H(e_k)\| = T_s \max\left\{f_3\sqrt{e_{1,k}^2 + e_{2,k}^2}, \sqrt{\left(1+f_1^2\right)\left(e_{3,k}^2 + e_{4,k}^2\right)}\right\}.$$

Multiplying the numerator and the denominator of the last equation by $\|e_k\| = \sqrt{\sum_{i=1}^{6} e_{i,k}^2}$, observing that

$$\max\left\{\sqrt{e_{1,k}^2 + e_{2,k}^2} + \sqrt{e_{3,k}^2, e_{4,k}^2}\right\} \leq \|e_k\|$$

and, finally, choosing $\alpha = T_s \max\{f_3, \sqrt{1+f_1^2}\}$, yields (7). □

Proof of Proposition 3: From (5)–(7), the following inequality holds:

$$\|f(x_k) - f(\hat{x}_k)\| \leq \|J(\hat{x}_k)\| \|e_k\| + \|H(e_k)\| \|e_k\|$$

and using (6) and (7), (9) is obtained. □

Proof of Proposition 4: The relation directly follows from (6). □

Proof of Proposition 5: By Proposition 2, it results $A_k = A + J(\hat{x}_k) = A + \sum_{i=1}^{5} J_i \hat{x}_{i,k}$. □

Proof of Proposition 6: Function $\hat{f}_c(x)$ can be written as $\hat{f}_c(x) = (M_1 x_1 + M_2 x_2 + M_3 x_3)x$, where $M_1 = (0,0,0,m_1,0,0)$, $M_2 = (0,0,0,-m_1,0,0)$, and $M_3 = (0,0,m_2,m_3,0,0)$, with $m_1 = (0,0,0,0,-f_3,0)^T$, $m_2 = (0,f_1,0,0,0,0,0)^T$, and $m_3 = (f_1,0,-1,0,-f_3,0)^T$. Consequently, we have

$$\left\|\hat{f}_c(x)\right\|_2 \leq \left(f_3\left(|x_1| + |x_2|\right) + \sqrt{1+f_1^2}|x_5|\right)\|x\| \leq \hat{\alpha}\left(|x_1| + |x_2| + |x_5|\right)$$

with $\hat{\alpha} = \alpha/T_s$ and α as in Proposition 2. Finally, we have $\|\hat{f}_c(x)\|_2 \leq 3\hat{\alpha}\|x\|^2$ because of $|x_i| \leq \|x\|$ for all i. □

Proof of Proposition 7: In [19], it is shown that the filter's gain matrix K_k is s.t. $\|K_k\| \leq N\overline{p}/\underline{r}$, for all k, where N is a suitable positive number. Consequently, since $\|C\| = 1$, we have $\|A_{s,k}\| \leq \|A_k\| + \|K_k\|\|C\| \leq N(1 + (\overline{p}/\underline{r})) = S$. □

REFERENCES

[1] R. Marino, P. Tomei, and C. Verrelli, "An adaptive tracking control from current measurements for induction motors with uncertain load torque and rotor resistance," *Automatica*, vol. 44, no. 10, pp. 2593–2599, Oct. 2008.

[2] B. Castillo-Toledo, S. Di Gennaro, A. Loukianov, and J. Rivera, "Discrete time sliding mode control with application to induction motors," *Automatica*, vol. 44, no. 12, pp. 3036–3045, Dec. 2008.

[3] F. Alonge and F. D'Ippolito, "Design and sensitivity analysis of a reduced-order rotor flux optimal observer for induction motor control," *Control Eng. Practice*, vol. 15, no. 12, pp. 1508–1519, Dec. 2007.

[4] C. Korlinchak and M. Comanescu, "Sensorless field orientation of an induction motor drive using a time-varying observer," *IET Elect. Power Appl.*, vol. 6, no. 6, pp. 353–361, Jul. 2012.

[5] Y.-R. Kim, S.-K. Sul, and M.-H. Park, "Speed sensorless vector control of induction motor using extended Kalman filter," *IEEE Trans. Ind. Appl.*, vol. 30, no. 5, pp. 1225–1233, Sep./Oct. 1994.

[6] F. Alonge, F. D'Ippolito, A. Fagiolini, and A. Sferlazza, "Extended complex Kalman filter for sensorless control of an induction motor," *Control Eng. Practice*, vol. 27, pp. 1–10, May 2014.

[7] S. Jafarzadeh, C. Lascu, and M. S. Fadali, "State estimation of induction motor drives using the unscented Kalman filter," *IEEE Trans. Ind. Electron.*, vol. 59, no. 11, pp. 4207–4216, Nov. 2012.

[8] M. Barut, R. Demir, E. Zerdali, and R. Inan, "Real-time implementation of bi input-extended Kalman filter-based estimator for speed-sensorless control of induction motors," *IEEE Trans. Ind. Electron.*, vol. 59, no. 11, pp. 4197–4206, Nov. 2012.

[9] F. Alonge, F. D'Ippolito, and A. Sferlazza, "Sensorless control of induction motor drive based on roust Kalman filter and adaptive speed estimation," *IEEE Trans. Ind. Electron.*, vol. 61, no. 3, pp. 1444–1453, Mar. 2014.

[10] F. D'Ippolito, F. Alonge, and A. Sferlazza, "Descriptor-type robust Kalman filter and neural adaptive speed estimation scheme for sensorless control of induction motor drive systems," *Robust Control Des.*, vol. 7, no. 1, pp. 51–56, 2012.

[11] J. Holtz, "Sensorless control of induction motor drives," *Proc. IEEE*, vol. 90, no. 8, pp. 1359–1394, Aug. 2002.

[12] R. Vieira, C. Gastaldini, R. Azzolin, and H. Grundling, "Sensorless sliding mode rotor speed observer of induction machines based on magnetizing current estimation," *IEEE Trans. Ind. Electron.*, vol. 61, no. 9, pp. 4573–4582, Sep. 2014.

[13] S. M. Gadoue, D. Giaouris, and J. W. Finch, "MRAS sensorless vector control of an induction motor using new sliding-mode and fuzzy-logic adaptation mechanisms," *IEEE Trans. Energy Convers.*, vol. 25, no. 2, pp. 394–402, Jun. 2010.

[14] C. Canudas De Wit, A. Youssef, J. Barbot, P. Martin, and F. Malrait, "Observability conditions of induction motors at low frequencies," in *Proc. IEEE Conf. Decision Control*, 2000, vol. 3, pp. 2044–2049.

[15] S. Ibarra-Rojas, J. Moreno, and G. Espinosa-Pérez, "Global observability analysis of sensorless induction motors," *Automatica*, vol. 40, no. 6, pp. 1079–1085, Jun. 2004.

[16] P. Vaclavek, P. Blaha, and I. Herman, "AC drives observability analysis," *IEEE Trans. Ind. Electron.*, vol. 60, no. 8, pp. 3047–3059, Aug. 2013.

[17] T. Du, P. Vas, and F. Stronach, "Design and application of extended observers for joint state and parameter estimation in high-performance ac drives," *Proc. Inst. Elect. Eng.–Elect. Power Appl.*, vol. 142, no. 2, pp. 71–78, Mar. 1995.

[18] M. Barut, S. Bogosyan, and M. Gokasan, "Speed-sensorless estimation for induction motors using extended Kalman filters," *IEEE Trans. Ind. Electron.*, vol. 54, no. 1, pp. 272–280, Feb. 2007.
[19] K. Reif, S. Gunther, E. Yaz, and R. Unbehauen, "Stochastic stability of the discrete-time extended Kalman filter," *IEEE Trans. Autom. Control*, vol. 44, no. 4, pp. 714–728, Apr. 1999.
[20] T.-J. Tarn and Y. Rasis, "Observers for nonlinear stochastic systems," *IEEE Trans. Autom. Control*, vol. 21, no. 4, pp. 441–448, Aug. 1976.
[21] F. Alonge, T. Cangemi, F. D'Ippolito, and G. Giardina, "Speed and rotor flux estimation of induction motors via on-line adjusted extended Kalman filter," in *Proc. 32nd Annu IEEE IECON*, Nov. 2006, pp. 336–341.
[22] R. Marino, P. Tomei, and C. M. Verrelli, *Induction Motor Control Design*. New York, NY, USA: Springer-Verlag, 2010.
[23] P. Vas, *Sensorless Vector and Direct Torque Control*. Oxford, U.K.: Oxford Univ. Press, 1998.
[24] P. Alkorta, O. Barambones, J. Cortajarena, and A. Zubizarreta, "Efficient multivariable generalized predictive control for sensorless induction motor drives," *IEEE Trans. Ind. Electron.*, vol. 61, no. 9, pp. 5126–5134, Sep. 2014.

Francesco Alonge (M'02) was born in Agrigento, Italy, in 1946. He received the Laurea degree in electronic engineering from the University of Palermo, Palermo, Italy, in 1972.

Since then, he has been with the University of Palermo, where he is currently a Full Professor of automatic control with the Department of Energy, Information Engineering, and Mathematical Models. His research topics include electrical drive control (including linear and nonlinear observers, stochastic observers, parametric identification), robot control, parametric identification and control in power electronics, and UAV motion control in aeronautics.

Tommaso Cangemi received the M.S. degree in computer science engineering and the Ph.D. degree in automatic control engineering from the University of Palermo, Palermo, Italy, in 2003 and 2007, respectively.

From 2007 to 2009, he was with the Department of Automation, University of Palermo, where he assisted and worked in the field of electrical motor drives, optimum control, and internal models. Currently, he is a Consultant with Altran Italia S.p.A., Rome, Italy. He works on the development of projects in the field of automatic control and software embedded for automotive and power electronics.

Filippo D'Ippolito (M'00) was born in Palermo, Italy, in 1966. He received the Laurea degree in electronic engineering and the Research Doctorate degree in systems and control engineering from the University of Palermo, Palermo, in 1991 and 1996, respectively.

He is currently a Research Associate with the Department of Energy, Information Engineering, and Mathematical Models, University of Palermo. His research interests include control of electrical drives, control of electrical power converters, adaptive and visual/force control of robot manipulators, rehabilitation robotics, and marine robotics.

Dr. D'Ippolito received the 2000 Kelvin Premium from the Institution of Electrical Engineers, U.K., for the paper "Parameter identification of induction motor model using genetic algorithms."

Adriano Fagiolini (M'05) received the Laurea degree in computer science engineering and the Ph.D. degree in robotics and automation from the University of Pisa, Pisa, Italy, in 2004 and 2009, respectively. He was a summer student at the European Center for Nuclear Research (CERN), Geneva, Switzerland. He enrolled in the International Curriculum Option of doctoral studies in hybrid control for complex, distributed, and heterogeneous embedded systems.

He is currently an Assistant Professor with the University of Palermo, Palermo, Italy.

Dr. Fagiolini led the University of Pisa's team at the first European Space Agency's Lunar Robotics Challenge, which resulted in a second place prize for the team. His research interests include Boolean and Set-valued consensus and intrusion detection in distributed multirobot systems.

Antonino Sferlazza (S'12) was born in Palermo, Italy, in November 1987. He received the Master's degree in automation engineering in 2011 from the University of Palermo, Palermo, where he is currently working toward the Ph.D. degree in system and control engineering in the Department of Energy, Information Engineering, and Mathematical Models.

His research interests include the development of feedback control algorithms for nonlinear dynamical systems, optimization techniques, estimation of stochastic dynamical systems, and applications of control of electrical drives, power converters, and mechanical systems.